



## **Hydrogeochemical modeling and groundwater quality in coastal aquifers in Northeastern Brazil**

**ARTICLES** doi:10.4136/ambi-agua.3082

**Received: 17 May 2025; Accepted: 29 Aug. 2025**

**Karen Vendramini de Araújo<sup>1\*</sup> ; Itabaraci Nazareno Cavalcante<sup>2</sup> ;  
Diolande Ferreira Gomes<sup>1</sup> ; Rafael Mota de Oliveira<sup>3</sup> ;  
Letycia Oliveira Venâncio<sup>4</sup> ; João Capistrano de Abreu Neto<sup>5</sup> ;  
Gisele Simone Lopes<sup>6</sup> ; Narelle Maia de Almeida<sup>1</sup> **

<sup>1</sup>Departamento de Geologia. Laboratório de Geologia e Geofísica Marinha e Aplicada à Energia. Universidade Federal do Ceará (UFC), Campus do Pici, Blocos 912 e 913, CEP: 60440-900, Fortaleza, CE, Brazil.

E-mail: dfreire68@gmail.com, narelle@ufc.br

<sup>2</sup>Departamento de Geologia. Laboratório de Hidrogeologia. Universidade Federal do Ceará (UFC), Campus do Pici, Bloco 913, CEP: 60440-900, Fortaleza, CE, Brazil. E-mail: itabaracicavalcante@gmail.com

<sup>3</sup>Companhia de Gestão dos Recursos Hídricos (COGERH), Rua Aualdo Batista, nº 1550, CEP: 60824-140, Fortaleza, CE, Brazil. E-mail: rafaelmotageo@gmail.com

<sup>4</sup>Instituto de Geociências. Universidade Estadual de Campinas (UNICAMP), Rua Carlos Gomes, nº 250, Cidade Universitária, CEP: 13083-855, Campinas, SP, Brazil. E-mail: letycia.venancio@hotmail.com

<sup>5</sup>Instituto Federal de Pernambuco (IFPE), Campus Pesqueira, BR- 232, s/n, CEP: 55360000, Pesqueira, PE, Brazil. E-mail: joaoabreuneto@gmail.com

<sup>6</sup>Departamento de Química Analítica e Físico-Química. Universidade Federal do Ceará (UFC), Campus do Pici, Bloco 940, CEP: 60440-900, Fortaleza, CE, Brazil. E-mail: gslopes@ufc.br

\*Corresponding author. E-mail: karenva83@gmail.com

**Editor-in-Chief: Nelson Wellausen Dias **

### **ABSTRACT**

Geochemical modeling is a central approach in hydrogeochemical assessments, enabling the identification of water-rock equilibrium conditions through mineral saturation indices and thereby increasing understanding of processes that control the chemical characteristics of groundwater. This study identified the main mechanisms governing hydrogeochemical behavior and evaluated the equilibrium conditions of the mineral species that comprise the hydrogeological framework of the northeastern coast of Brazil, using geochemical modeling to infer the processes controlling compositional and qualitative aspects from groundwater potable standards. The results indicate a predominance of sodium-chloride waters with concentrations of total dissolved solids, chloride, total hardness, sulfate, sodium, total iron, nitrate, turbidity, barium, and lead outside potable standards. Weathering induced by the interaction between groundwater and minerals of the infiltrated aquifers emerges as the principal hydrogeochemical control factor in the area. Geochemical modeling shows supersaturation for quartz, goethite, and hematite, and subsaturation for kaolinite, muscovite, illite, and calcite in the analyzed samples, explaining the high concentrations of elements from minerals prone to dissolution and the consequent addition of ions to solution, as well as the low concentrations of elements from minerals prone to precipitation, which are removed from solution. It is concluded that silicate weathering and carbonate dissolution are the main processes controlling the compositional state of groundwater in the region, with contributions from anthropogenic activities and marine influence.



**Keywords:** contamination, Gibbs diagram, phreeqc, Potiguar Basin.

## Modelagem hidrogeoquímica e qualidade das águas subterrâneas em aquíferos costeiros no Nordeste do Brasil

### RESUMO

A modelagem geoquímica é uma abordagem central em avaliações hidrogeoquímicas, permitindo identificar condições de equilíbrio água/rocha por meio de índices de saturação mineral e, assim, compreender os processos que controlam as características químicas das águas subterrâneas. Este estudo teve como objetivo identificar os principais mecanismos que governam o comportamento hidrogeoquímico e avaliar as condições de equilíbrio das espécies minerais que compõem o arcabouço hidrogeológico da região costeira do nordeste do Brasil, utilizando modelagem geoquímica para inferir os processos de controle composicional e qualitativo, a partir dos padrões de potabilidade das águas subterrâneas. Os resultados indicam predominância de águas cloretadas sódicas com concentrações de sólidos totais dissolvidos, cloreto, dureza total, sulfato, sódio, ferro total, nitrato, turbidez, bário e chumbo fora dos padrões de potabilidade. O intemperismo induzido pela interação entre águas subterrâneas e minerais dos aquíferos percolados emerge como o principal fator de controle hidrogeoquímico na área. A modelagem hidrogeoquímica aponta condições de supersaturação para quartzo, goethita e hematita, e de subsaturação para caulinita, muscovita, ilita e calcita nas amostras analisadas, justificando as altas concentrações de elementos provenientes de minerais propensos à dissolução e o acréscimo de íons em solução, bem como as baixas concentrações de elementos oriundos de minerais propensos à precipitação, que são removidos da solução. Conclui-se que o intemperismo de silicatos e a dissolução de carbonatos são os principais processos de controle composicional das águas subterrâneas da região, com contribuições de atividades antrópicas e da influência marinha.

**Palavras-chave:** Bacia Potiguar, contaminação, diagrama de Gibbs, phreeqc.

### 1. INTRODUCTION

Hydrogeochemical studies are essential for understanding the processes that control the chemical composition and quality of groundwater. They allow for the evaluation of associations between the identified constituents and interactions with the substrate, as well as the identification of potential relations with other environmental variables such as seasonal changes in aquifer recharge dynamics, anthropogenic activities and marine influence, in the case of coastal aquifers.

Geochemical modeling is one of the most applied approaches in hydrogeochemical assessments and consists of the mathematical representation of information through the use of computer programs, such as Phreeqc (Parkhurst and Appelo, 2013). One of the most widely used models is the mineral speciation and solubility model, which provides information about mineral species in solution and the saturation indexes (or states) of minerals (Venâncio *et al.*, 2020; Gomes *et al.*, 2021).

Generally, a chemical analysis provides total concentrations of elements in solution. A speciation calculation distributes these totals among chemical species using an aqueous model. The results of the speciation calculation are the activities of all aqueous species, which are used to calculate mineral saturation indexes relative to water (Parkhurst and Appelo, 2013).

Saturation indexes are used to assess the degree of equilibrium between water and the respective mineral. However, there is often no equilibrium, and the saturation state only indicates the direction in which reactions can occur. Thus, for undersaturation, dissolution is

expected, while supersaturation suggests precipitation (Appelo and Postma, 2005). Changes in saturation state are also useful for distinguishing the different stages of hydrogeochemical evolution and help identify which geochemical reactions are important in controlling the chemical composition of water (Coetsiers and Walraevens, 2006).

Accordingly, this study identified the main mechanisms responsible for hydrogeochemical behavior, considering the seasonal variations in recharge dynamics for aquifers and their contributions to the chemical characteristics of groundwater, and evaluated the equilibrium conditions of the mineral species that make up the hydrogeological framework of the area, through geochemical modeling, to infer the processes of compositional and qualitative control of groundwater in the northeastern coastal region of Brazil.

## 2. MATERIAL AND METHODS

The study area is located in the Icapuí municipality in the extreme east of the state of Ceará, Brazil (Figure 1). Water supply in the municipality is exclusively carried out through tubular wells managed by the Autonomous Water and Sewage Service (SAAE) and private wells. The municipality also does not have a sewage system; therefore, domestic sewage is collected through septic tanks.

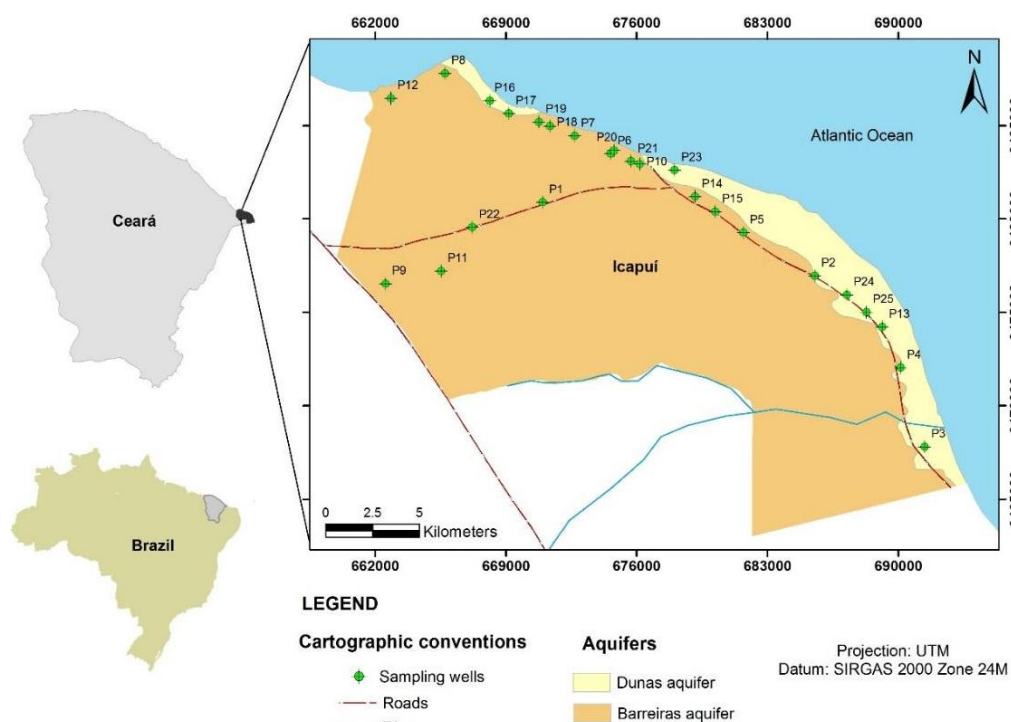


**Figure 1.** Distribution of sampled wells and hydrogeological units in the study área.  
**Source:** Serviço Geológico do Brasil (2014, modified).

The region is located in the hydrogeological context of the Coastal Province and Potiguar Subprovince, represented by the Dunas, Barreiras, Jandaíra, and Açú Aquifers (Mente, 2008).

The Dunas Aquifer is formed by Quaternary eolian deposits that occur along the entire coastal strip, with thicknesses ranging from 6 to 20 meters, according to the construction profiles and lithology of the wells existing in the study area.

The Barreiras Aquifer is composed of clasts of ages ranging from the Miocene to the Pliocene-Pleistocene that outcrop in most of the study area, but also occur underlying the Dunas Aquifer.

The Jandaíra and Açú Aquifers are composed of Cretaceous sediments of the Apodi Group

(Soares *et al.*, 2003). From construction profiles and lithology of the wells existing in the area, it was possible to identify that the Jandaíra Aquifer occurs at depths ranging from 20 to 108 meters, with the upper contact concordant with the Barreiras Aquifer and the lower with the Açú Aquifer. In the extreme west of the study area, the carbonate rocks of the Jandaíra Formation outcrop at the base of the Barreiras Formation cliffs in the form of small slabs restricted to the beach zone.

The Açú Aquifer is detected in the area at depths greater than 200 meters, as observed in construction profiles and lithology of the wells and corresponds to the lower portion of the Açú Formation which, according to Braga Júnior *et al.* (2017), presents conglomerates at the base, changing to coarse sandstones and at the top floodplain deposits. It occurs under confined conditions, both by the clay layers of the upper portion of the Açú Formation and by the base of the Jandaíra Aquifer.

Physicochemical analysis data from 50 groundwater samples collected from 25 wells in the municipality of Icapuí, Ceará (Figure 1) were used. The wells were selected based on criteria such as distribution in the area, access to the sampling point, water use, and the aquifers tapped. Sampling was conducted during two campaigns in February (rainy season) and August (dry season) of 2019.

The collected samples were subjected to physicochemical analyses, including pH, electrical conductivity, total dissolved solids, total alkalinity, bicarbonate, carbonate, chloride, calcium, magnesium, total hardness, sulfate, sodium, potassium, total iron, silica, nitrate, nitrite, ammonia, turbidity, fluoride, and bromide. The analyses were performed by the Environmental Geochemistry Laboratory of the Federal University of Ceará using the methodology established by the Standard Methods for the Examination of Water and Wastewater (APHA *et al.*, 2012). Trace metals (aluminum, barium, copper, iron, manganese, nickel, lead, and zinc) and dissolved phosphorus were analyzed by Inductively Coupled Plasma Optical Emission Spectrometry (ICP-OES), performed by the Ceará Nucleus of Technology and Industrial Quality (NUTEC), from samples vacuum filtered using a 0.45 µm porosity membrane.

The iron present in the samples was analyzed in two forms, total and dissolved. Total iron was used for the evaluation of potability, as it has a reference value established by the legislation adopted in this study, and dissolved iron was used in the Phreeqc modeling, due to the ICP-OES technique allowing the detection of elements that occur in low concentrations.

The results of the physicochemical analyses were compared with Ordinance No. 888/2021 of the Ministry of Health (Brasil, 2021) to assess suitability for human consumption. Classification according to the dominant ionic content was done using the Piper diagram, constructed using the Qualigraf software (Mobüs, 2003).

The main geochemical processes that contribute to the chemical characteristics of groundwater were identified using the Gibbs diagram (Gibbs, 1970), which defines precipitation, rock weathering, and the evaporation process as the main natural mechanisms that control water chemistry. The evaluation of the waters is done based on the relation between total dissolved solids and the ratios  $rNa^+/r(Na^+ + Ca^{2+})$  and  $rCl^-/r(Cl^- + HCO_3^-)$ , where "r" indicates that the concentrations of  $Na^+$ ,  $Ca^{2+}$ ,  $Cl^-$ , and  $HCO_3^-$  are expressed in meq/L.

Sediment and rock samples were also collected for X-ray diffraction analysis by the Structural Crystallography Laboratory of the Federal University of Ceará. Four samples were analyzed, one from each of the main aquifers in the area (Dunas, Barreiras, Jandaíra, and Açú) to identify the mineralogical compositions, from which saturation indexes were calculated using the Phreeqc software (Version 3.5).

Phreeqc allows the simulation of various reactions and processes that occur in natural environments, resulting from interactions between water and the geological environment. For this reason, it has been used in several hydrogeochemical studies around the world with a wide variety of applications (Venâncio *et al.*, 2020).

In this study, the mineral speciation and solubility model was applied using the Wateq4f thermodynamic database due to its better suitability for the analyzed ions. The saturation index (SI) obtained from the model was used to assess the degree of equilibrium between water and mineral phases. The SI is defined by the ratio between the Ion Activity Product (IAP) and the Solubility Product (SP) as shown in Equation 1 (Garrels and Christ, 1965):

$$SI = \log_{10} (K_{IAP}/K_{SP}) \quad (1)$$

Based on the value of SIs, it was possible to identify the saturation states of minerals as equilibrium or saturation ( $SI=0$ ), undersaturation ( $SI<0$ ) or supersaturation ( $SI>0$ ). As a result, saturation states of minerals indicate the directions of geochemical processes. Thus, undersaturation indicates a tendency towards dissolution and supersaturation indicates a tendency towards precipitation of the mineral phase, while the state of equilibrium or saturation indicates that the mineral can dissolve or precipitate to remain in equilibrium in the solution. In practice, the interval  $-0.05<SI<0.05$  is considered to be in equilibrium (Parkhurst and Appelo, 2013).

### 3. RESULTS AND DISCUSSION

#### 3.1. Chemical and Qualitative Characteristics of Groundwater

Groundwater tends to increase the concentrations of dissolved substances as it percolates through different aquifers; however, factors such as climate, recharge water composition, and anthropogenic activities can also cause these concentrations to increase.

Based on the analytical results of the 50 collected samples, it was possible to identify the chemical characteristics and quality, based on the standards for human consumption of groundwater in each seasonal period.

The waters present a neutral to slightly acidic tendency, for both the rainy and dry periods, with average pH values of  $6.6 \pm 0.9$  and  $6.3 \pm 1.0$ , respectively, with a slight decrease in pH in the dry period. Samples P9 and P22 present an alkaline pH, around 8, distant from the average, suggesting waters of a different hydrochemical type from the others. Total alkalinity is represented by bicarbonates and also does not show significant variations between the seasonal periods, with averages of  $111.7 \pm 91.9$  (rainy season) and  $106.5 \pm 96.7$  mg L<sup>-1</sup> (dry season).

According to the dominant ionic content, the groundwater in the area presents three hydrochemical facies. Of these, 22 samples (88%) represent sodium chloride waters; 2 samples (8%) are sodium bicarbonates; and 1 sample (4%) is calcium chloride, for both seasonal periods (Figure 2).

The predominance of sodium chloride waters is mainly associated with the capture of the Dunas and Barreiras Aquifers. The unconfined nature of these aquifers makes them more susceptible to the leaching of salts, originating from marine aerosols deposited in the soil, as well as the infiltration of water from coastal lagoons, often brackish due to the process of evaporation and salt concentration.

The samples that present sodium bicarbonate waters were collected in wells P9 and P22 located in the region farthest from the coast, which have depths of 370 and 685 meters, respectively, capturing deep aquifer levels associated mainly with the sandy layers of the Açú Formation.

The calcium chloride hydrochemical facies was identified in the samples collected in well P11, which has a depth of 594 meters and also captures from the Açú Aquifer.

The presence of Ca<sup>2+</sup> and HCO<sub>3</sub><sup>-</sup> ions in the waters from the Açú Aquifer indicates a contribution from the overlying Jandaíra Formation limestones, through the vertical percolation of waters enriched by the dissolution of CaCO<sub>3</sub>.

Regarding the quality of groundwater for human consumption, some parameters do not



conform with potability standards established by the Ministry of Health Ordinance No. 888/2021 (Brasil, 2021).

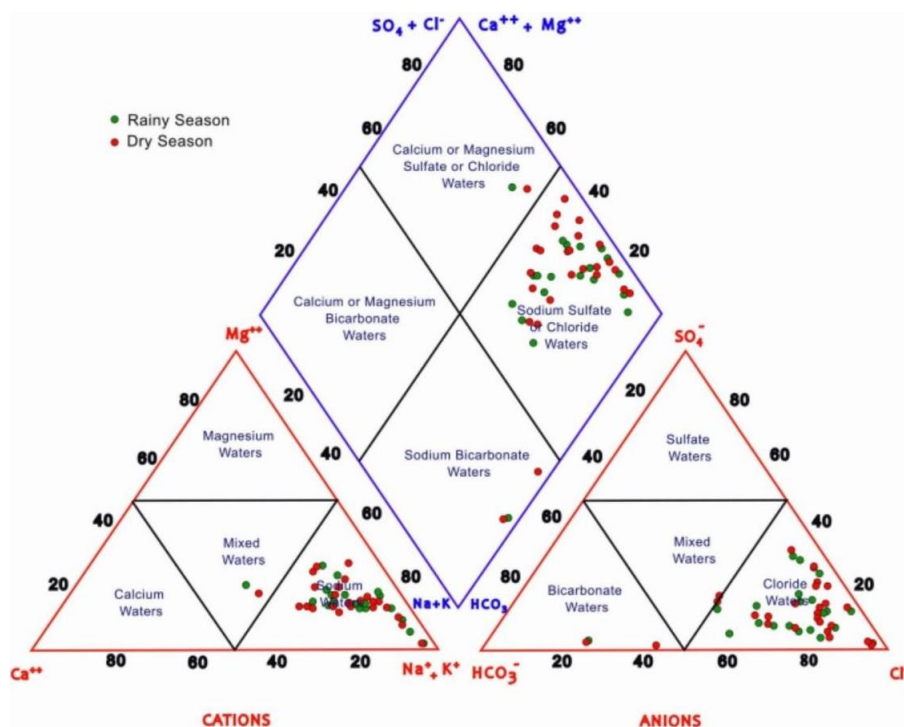


**Figure 2.** Ionic classification of groundwater in the study area.

Source: Möbius (2003).

Concentrations of total dissolved solids are above  $500 \text{ mg L}^{-1}$  (maximum permissible limit) for human consumption in about 60% of the samples in both seasonal periods. Regarding chloride, the influence of seasonality on sample values can be observed, as in the rainy season the values ranged from 30 to  $1189 \text{ mg L}^{-1}$  and in the dry season from 46 to  $1279 \text{ mg L}^{-1}$ . For both periods, more than 50% of the samples showed values above the maximum permissible limit (MPL) of  $250 \text{ mg L}^{-1}$  for chloride in drinking water.

Total hardness, obtained from the concentrations of  $\text{Ca}^{2+}$  and  $\text{Mg}^{2+}$ , is expressed as  $\text{CaCO}_3$  content. According to Custódio and Llamas (1983), waters, in relation to hardness, are classified as soft ( $< 50 \text{ mg L}^{-1} \text{ CaCO}_3$ ), slightly hard ( $50 - 100 \text{ mg L}^{-1} \text{ CaCO}_3$ ), hard ( $100 - 200 \text{ mg L}^{-1} \text{ CaCO}_3$ ) and very hard ( $> 200 \text{ mg L}^{-1} \text{ CaCO}_3$ ). In approximately 60% of the analyzed samples, the waters were classified as hard or very hard, in both seasonal periods. The MPL of  $300 \text{ mg L}^{-1}$  for total hardness in water intended for human consumption was exceeded in about 20% of the samples, in both the rainy and dry seasons. The higher occurrence of hard and very hard waters in the area can be attributed to the interaction with the carbonate rocks of the Jandaíra Formation.

Sulfate concentrations varied from 0.6 to  $288.5 \text{ mg L}^{-1}$  in the rainy season and 0.4 to  $224.1 \text{ mg L}^{-1}$  in the dry season. Only sample P23 exceeded the maximum permissible limit of  $250 \text{ mg L}^{-1}$  for drinking water, and it was collected during the rainy season, possibly associated with the infiltration of recent rainwater. According to Celligoi (1999), significant amounts of sulfate are added to the hydrological cycle through atmospheric precipitation, coming from, among other sources, marine aerosols. Like sulfate, sodium showed higher concentrations in the rainy season, but with values above the drinking water standards ( $200 \text{ mg L}^{-1}$ ) in both periods, with about 40% in the rainy season and 30% in the dry season. For the fluoride ion, all samples were within the drinking water standards ( $1.5 \text{ mg L}^{-1}$ ) in both seasonal periods.

Regarding total iron, only sample P9 showed a concentration above the maximum

permissible limit of  $0.3 \text{ mg L}^{-1}$ , with  $0.6 \text{ mg L}^{-1}$  during the dry season, which may be associated with the lateritic levels present in the Barreiras Formation. Turbidity, a parameter associated with suspended solids in water, showed values within the drinking water standards in most of the samples, with higher values occurring during the rainy season, which may be related to the transport of material, such as clay, silt, or organic matter, promoted by rainwater recharge. However, sample P9 showed a value of 8.3 uT, above the MPL of 5 uT for turbidity, during the dry season, which may be associated with the presence of particulate iron, considering that this sample also has the highest concentration of total iron in the same period.

Regarding nitrogen compounds, the ammonia concentrations are below the maximum permissible limit ( $1.2 \text{ mg L}^{-1}$  as  $\text{N-NH}_{3,4}$ ) for both the rainy and dry seasons. However, for nitrate, concentrations exceed the MPL in both periods. The lack of basic sanitation in the area, combined with the predominance of sandy aquifers, which are naturally more vulnerable to pollutant percolation, contributes to the increase in nitrate concentrations in the water. The maximum permissible limit for nitrate in drinking water in Brazil ( $10 \text{ mg L}^{-1}$  as  $\text{N-NO}_3^-$ ) is slightly more restrictive than the World Health Organization (WHO) guideline of  $50 \text{ mg L}^{-1}$  as  $\text{NO}_3^-$  or  $11.3 \text{ mg L}^{-1}$  as  $\text{N-NO}_3^-$ . In the rainy season, 3 of the 25 samples showed values above  $10 \text{ mg L}^{-1}$  of  $\text{N-NO}_3^-$ , while in the dry season 8 samples were above the MPL. The increase in nitrate concentrations in the dry season is probably due to the lower volume of precipitation, which interferes with the dilution of this parameter promoted by rainwater recharge.

Regarding trace metals, the concentrations of aluminum, copper, manganese, nickel, and zinc did not show significant anomalies, with all samples within the drinking water standards. However, the concentrations of barium and lead showed values above the maximum allowed by the Ministry of Health of  $0.7$  and  $0.01 \text{ mg L}^{-1}$ , respectively. In the rainy season, barium values reached  $0.8 \text{ mg L}^{-1}$  and lead showed a maximum of  $0.01 \text{ mg L}^{-1}$ . In the dry season, barium and lead concentrations reached  $0.9$  and  $0.02 \text{ mg L}^{-1}$ , respectively. Maia *et al.* (2018) attributes the presence of lead in the groundwater of the region to natural sources, mainly the lateritic layer of the Barreiras Formation. Geochemical analyzes carried out by Souza (2017) on the sediments and laterites of the Barreiras Formation in the cliffs of the region showed lead in concentrations up to twice as high as the average values defined by Turekian and Wedepohl (1961) for sandstones, which is 7 ppm. Barium is also attributed to natural sources, being associated with both the sandstones of the Barreiras Formation and the carbonates of the Jandaíra Formation. Considering that the concentrations found by Souza (2017) in the sediments of both formations were also higher than the average values defined by Turekian and Wedepohl (1961).

### 3.2. Mineralogy of the Aquifers

The mineralogical framework of the geological units in the area is composed essentially of silicates, carbonates, oxides, and oxyhydroxides. The mineralogy was identified from the diffractograms of rock and sediment samples that make up the four main aquifers (Figure 3).

The dune sediments that make up the Dune Aquifer are composed essentially of quartz with subordinate kaolinite (Figure 3a). According to Maia *et al.* (2018), the dunes in the study area are formed by quartz and/or quartz-feldspathic sands and, being an older generation of dunes, present the development of pedogenic processes.

The lateritic sandstones that make up the Barreiras Aquifer present predominant quartz, subordinate kaolinite, and accessory amounts of goethite and hematite (Figure 3b). According to Souza (2017), quartz and kaolinite come substantially from the erosion and alteration of rocks of granitic composition of the crystalline basement. They are, therefore, of pedogenic origin, as well as may have been reworked from the continental depositional system of the Barreiras Formation itself. Goethite and hematite are also of pedogenic origin, possibly integrated into the original sediments of the Barreiras Formation.

The carbonate rocks that form the Jandaíra Aquifer are composed essentially of calcite and

present quartz as an accessory mineral (Figure 3c). The presence of siliciclastic grains suggests a fluvial contribution at the time of deposition of these rocks (Sousa *et al.*, 2009).

The sandstones that make up the Açú Aquifer present predominant quartz, subordinate muscovite, kaolinite, illite, and accessory amounts of goethite and hematite (Figure 3d). According to Maraschin *et al.* (2010), the most frequent detrital constituent is quartz. Muscovite is concentrated in fine to médium grained sandstones and is often kaolinitized. The sandstones of the Açú Formation underwent intense diagenetic alterations that promoted the precipitation of kaolinite, illite-smectite, and iron oxides.

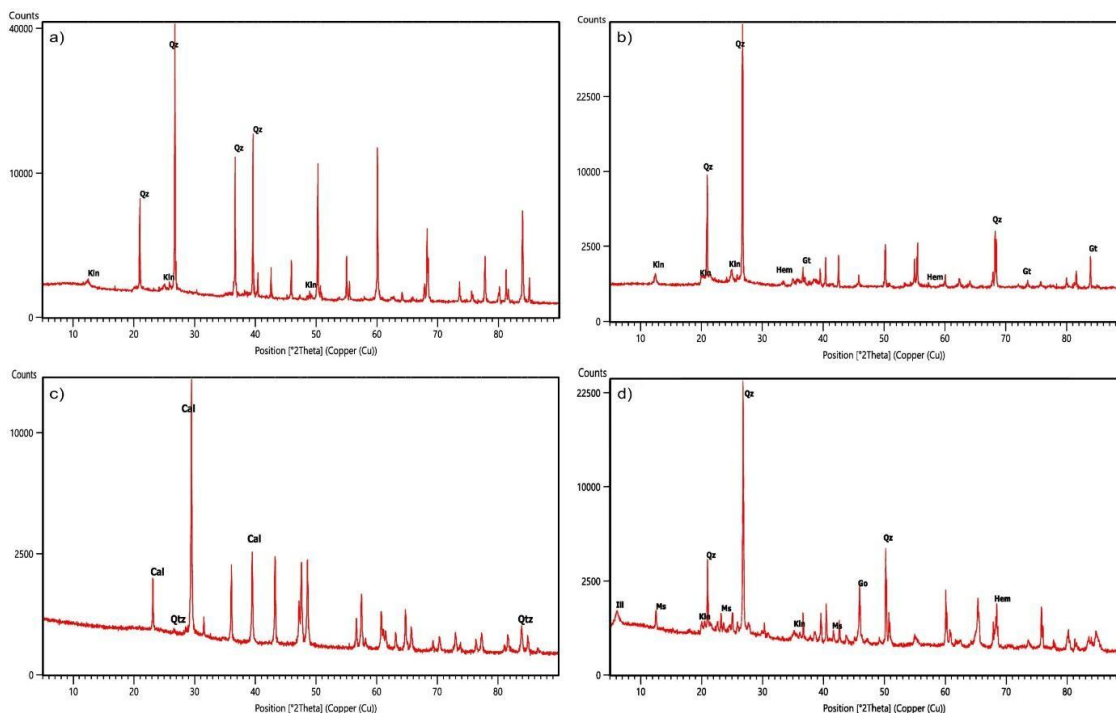


**Figure 3.** Diffractograms of rock and sediment samples of the aquifers in the study area. (a) Dune sediments; (b) Barreiras Formation; (c) Jandaíra Formation and (d) Açú Formation.

### 3.3. Hydrogeochemistry

The hydrogeochemistry in the area is predominantly controlled by weathering, promoted by the interaction between groundwater and the rocks that make up the percolated aquifers.

Figure 4 shows that the samples are in the weathering domain tending towards the limit of the evaporation domain, indicating characteristics of marine waters, that is, rich in sodium and poor in calcium, rich in chloride and poor in bicarbonate. However, the concentrations of these elements do not make the waters saline, in general they are fresh to slightly brackish, and therefore, with the exception of samples P13 and P23, they are not delimited in the domain of evaporated waters.

The  $rNa^+/rCl^-$  ratio of 0.817, for one of the two samples of well P13, is close to the ratio found for seawater, 0.858 (Richter and Kreitler, 1993), thus corroborating the result of the Gibbs diagram, which indicates a domain of evaporation process. Thus, a contribution of seawater to the recharge of the aforementioned well can be assumed, which presented the highest concentration in TDS ( $2631 \text{ mg L}^{-1}$ ) among all samples, especially after the dry period, or simply natural evolution in the process of water mineralization (water-rock interaction). The same discussion applies to well P23, whose samples have  $rNa^+/rCl^- = 0.810$  and which reach the limit of the weathering domain tending towards the evaporation domain in the Gibbs diagram.

The waters of well P11, together with those of wells P13 and P23, are the most brackish in



the area, where total dissolved solids exceed  $2000 \text{ mg L}^{-1}$ . However, these waters are not enriched in sodium relative to calcium, as observed for waters in the evaporation domain, and are therefore delimited in the domain of rocks, a process of water-rock interaction, but with a tendency towards salinization from one sampling to another, since the TDS concentration was  $1697 \text{ mg L}^{-1}$  (rainy season) to  $2227 \text{ mg L}^{-1}$  (dry season). This rapid change in the chemical composition of water may be related to intense pumping of the well, capturing water from other formations or deeper ones. A marine contribution in the drier period when the water level relative to the sea is lower can also be assumed.

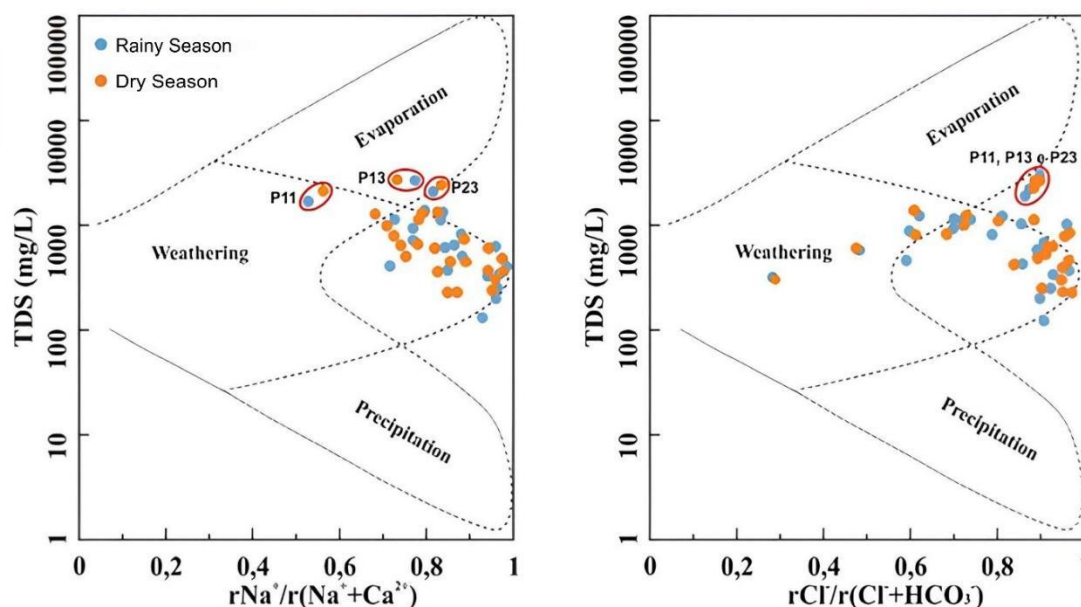


**Figure 4.** Natural mechanisms of hydrogeochemical control.

Source: Gibbs (1970).

### 3.3.1. Mineral Speciation and Solubility Modeling

The mineral speciation and solubility model, using the Phreeqc program, was initiated with the calculations of molar concentration, ionic activity, and activity coefficient of the chemical species present in the groundwater samples, from which the saturation indexes of the mineral phases identified in the aquifer formations were obtained.

The mineral phases analyzed in the modeling include silicates (quartz, kaolinite, muscovite, and illite), iron oxyhydroxide and oxide (goethite and hematite), and carbonate (calcite). Tables 1 and 2 show the saturation indexes of the aforementioned minerals and the pH levels in the groundwater in each seasonal period.

For silicates, quartz presented supersaturation conditions with positive saturation indexes in all samples and in both seasonal periods, indicating a tendency for the formation of the solid mineral phase (precipitation) from the solution. The pH conditions of the groundwater in the area, which vary from neutral to slightly acidic, favor this tendency for precipitation, considering that silica is poorly soluble at pH below 8, its solubility increasing in more alkaline media.

Kaolinite and muscovite (kmica) presented subsaturation conditions with negative saturation indexes, indicating a tendency for dissolution in 92% of the samples in the rainy season and 84% in the dry season. Samples P19 and P23 in the rainy season and P9, P15, P23, and P24 in the dry season were supersaturated in these minerals. The identical behavior for these minerals in all samples occurs because kaolinite is the main product of muscovite dissolution when potassium is completely leached; however, illite formation occurs if potassium remains.

**Table 1.** Mineral saturation indexes and pH in groundwater samples collected during the rainy season.

Sample	pH	Quartz	Kaolinite	Kmica	Illite	Calcite	Goethite	Hematite
P1	5.57	0.37	-0.89	-0.51	-5.25	-3.23	1.95	5.92
P2	7.27	0.59	-8.42	-10.47	-12.03	-0.38	5.45	12.90
P3	6.21	0.53	-8.46	-11.37	-13.15	-2.29	3.44	8.90
P4	7.21	0.56	-8.39	-10.30	-11.95	-0.19	0.26	2.53
P5	7.57	0.66	-8.87	-10.66	-11.99	-0.25	0.66	3.33
P6	6.73	0.47	-7.78	-10.06	-12.15	-2.95	-0.77	0.46
P7	5.88	0.50	-9.72	-13.88	-15.27	-2.80	1.91	5.83
P8	5.21	0.63	-13.36	-19.71	-19.80	-4.08	-5.35	-8.70
P9	8.17	0.33	-10.69	-13.08	-14.30	-0.39	7.16	16.33
P10	5.28	0.55	-13.85	-20.72	-20.81	-4.80	0.99	3.99
P11	7.00	0.34	-8.47	-10.76	-12.54	-0.01	4.94	11.89
P12	7.05	0.52	-8.17	-10.01	-11.76	-0.48	-0.07	1.87
P13	7.11	0.55	-8.27	-10.11	-11.78	-0.03	0.00	2.01
P14	5.19	0.62	-13.56	-20.37	-20.40	-5.30	0.45	2.92
P15	7.05	0.49	-8.19	-10.35	-12.19	-1.11	0.04	2.08
P16	7.02	0.74	-7.67	-9.34	-11.06	-0.56	5.11	12.22
P17	7.05	0.72	-7.75	-9.38	-11.13	-0.32	4.61	11.22
P18	5.95	0.81	-9.79	-13.61	-14.69	-2.75	1.50	5.01
P19	5.97	0.84	4.49	7.76	1.77	-2.50	2.83	7.66
P20	5.29	0.50	-13.84	-20.45	-20.51	-4.29	-0.27	1.46
P21	5.31	0.56	-12.96	-19.31	-19.63	-4.58	-4.98	-7.96
P22	8.18	0.34	-10.67	-13.55	-14.59	-0.58	0.73	3.47
P23	7.51	0.24	3.79	8.54	2.26	0.00	7.67	17.35
P24	6.96	0.62	-7.79	-9.58	-11.45	-0.84	-0.23	1.55
P25	7.17	0.60	-8.22	-10.02	-11.72	-0.33	0.20	2.40

**Source:** Prepared by the author.

**Table 2.** Mineral saturation indexes and pH in groundwater samples collected during the dry period.

Sample	pH	Quartz	Kaolinite	Kmica	Illite	Calcite	Goethite	Hematite
P1	5.28	0.38	-14.07	-20.57	-20.72	-3.59	0.94	3.88
P2	7.28	0.61	-8.40	-10.37	-11.96	-0.43	4.97	11.94
P3	6.20	0.54	-8.50	-11.43	-13.20	-2.31	2.79	7.59
P4	7.12	0.57	-8.20	-10.13	-11.85	-0.31	0.06	2.13
P5	7.32	0.71	-8.30	-10.01	-11.50	-0.41	5.79	13.59
P6	5.84	0.46	-10.03	-14.21	-15.66	-3.90	-3.41	-4.81
P7	5.79	0.50	-10.23	-14.59	-15.88	-2.86	1.94	5.89
P8	5.17	0.66	-1.84	-2.40	-6.53	-4.09	0.67	3.35
P9	8.12	0.38	0.78	3.75	-1.30	-0.44	7.87	17.74
P10	5.28	0.62	-0.50	-0.65	-5.23	-4.36	0.95	3.92
P11	7.02	0.38	-8.44	-10.87	-12.53	0.10	3.71	9.42
P12	6.90	0.60	-7.76	-9.55	-11.45	-0.43	4.89	11.78
P13	6.77	0.59	-7.61	-9.45	-11.32	-0.32	4.45	10.92
P14	4.47	0.61	-6.07	-9.58	-12.30	-5.38	-1.08	-0.15
P15	5.31	0.43	0.63	1.39	-3.80	-3.76	0.72	3.44
P16	6.86	0.42	-8.03	-10.17	-12.15	-0.67	4.71	11.43
P17	6.84	0.41	-8.03	-10.10	-12.11	-0.51	4.52	11.05
P18	5.53	0.50	-11.74	-17.06	-17.83	-3.14	0.84	3.70
P19	5.57	0.48	-11.54	-16.74	-17.60	-3.27	-4.25	-6.49
P20	5.15	0.50	-13.99	-20.84	-20.85	-4.39	0.19	2.39
P21	5.07	0.57	-13.30	-20.08	-20.31	-4.91	-5.70	-9.39
P22	7.95	0.36	-10.18	-13.12	-14.31	-0.67	6.09	14.20
P23	7.30	0.29	1.92	5.38	-0.12	-0.12	7.49	16.99
P24	6.73	0.65	5.45	10.05	3.61	-1.54	5.08	12.17
P25	7.02	0.39	-8.38	-10.55	-12.43	-0.41	-0.14	1.73

**Source:** Prepared by the author.

For illite, a similar behavior was identified, with a tendency for dissolution in 92% of the

samples in the rainy season and 96% in the dry season. In samples P19 and P23 in the rainy season and P24 in the dry season, illite shows a tendency to precipitate.

Variations in water input between the seasonal periods modify the pH conditions, as well as the solute/solvent equilibrium, promoting changes in the solubility of aluminosilicates and clays, represented by muscovite, kaolinite and illite in samples associated with the capture of the Dune and Barreiras Aquifers.

Regarding iron oxyhydroxides and oxides, the groundwater in the area is supersaturated in most of the analyzed samples, in both seasonal periods.

Goethite presents a supersaturation condition (precipitation) in 68% of the samples in the rainy season and 80% of the samples in the dry season. The subsaturation condition (dissolution) occurs in samples P6, P8, P12, P20, P21, and P24 in the rainy season and in samples P6, P14, P19, P21, and P25 in the dry season. In samples P13 and P15, goethite presents a saturation condition (dissolving or precipitating to remain in equilibrium in the solution) with saturation indexes between -0.05 and 0.05 in the rainy season.

Hematite shows a tendency to precipitate in 92% of the samples in the rainy season and 84% of the samples in the dry season. In samples P8 and P21 in the rainy season and P6, P14, P19, and P21 in the dry season, hematite presents a subsaturation condition, with a tendency to dissolve.

Goethite is normally formed under oxidizing conditions, accumulating by direct precipitation from seawater and meteoric waters. The formation of hematite is mainly related to metasomatism by solutions, but it can also form by chemical precipitation of colloidal  $\text{Fe}^{2+}\text{O}^{3-}$  and diagenetic alteration of iron-rich sediments (Deer *et al.*, 1992).

The greater tendency for precipitation identified for iron minerals is responsible for the occurrence of lateritic levels present along the cliffs of the Barreiras Formation in the area, considering that these levels are composed mainly of iron oxides and oxyhydroxides, such as hematites and goethite.

For the carbonate mineral phase existing in the area, represented by calcite, the predominance of the subsaturation condition is identified, with a tendency to dissolve in 88% of the samples in the rainy season and 96% in the dry season, with a tendency to precipitate in sample P11 in the dry season and a saturation condition (equilibrium) in samples P11, P13, and P23 in the rainy season.

Groundwater in the area tends to be neutral to slightly acidic, both in the rainy and dry seasons, favoring the dissolution of calcite in most samples. However, in sample P11, a tendency for precipitation occurs during the dry season, which may be associated with the influence of waters originating from the limestones that make up the Jandaíra Aquifer, which are rich in calcium, considering that sample P11, in both seasonal periods, presents the highest calcium concentrations in the area, exceeding  $200 \text{ mg L}^{-1}$ , whose averages are  $41.92 \text{ mg L}^{-1} \pm 49.22 \text{ mg L}^{-1}$  and  $47.2 \text{ mg L}^{-1} \pm 59.57 \text{ mg L}^{-1}$ , for the rainy and dry seasons, respectively.

## 4. CONCLUSIONS

The Icapuí region is characterized by alternating dry and rainy seasons, which directly influence aquifer recharge dynamics and can lead to variations in groundwater chemistry between periods. Groundwater in the area is predominantly of the sodium chloride type and exhibits a neutral to slightly acidic pH in both dry and rainy seasons. Several parameters exceeded the recommended drinking water standards in both seasons, including total dissolved solids, chloride, total hardness, sodium, nitrate, barium, and lead. Sulfate concentrations exceeded acceptable limits only during the rainy season, while total iron and turbidity exceeded standards primarily in the dry season.

The observed hydrochemical patterns are mainly driven by geochemical processes,

particularly weathering resulting from interactions between groundwater and the mineral constituents of the aquifer formations. Hydrogeochemical modeling indicated supersaturation with respect to quartz, goethite, and hematite, and undersaturation with respect to kaolinite, muscovite, illite, and calcite.

The predominance of supersaturation for iron oxyhydroxides and oxides explains the low concentrations of iron in solution, while the elevated concentrations of dissolved constituents such as silica, potassium, and calcium are associated with the undersaturation, and consequent dissolution, of aluminosilicates and the carbonate phase, particularly calcite.

Chloride, sodium, and sulfate concentrations are largely attributed to marine influence, whereas nitrate concentrations above regulatory limits suggest contamination from anthropogenic sources. This anthropogenic impact warrants particular concern, as nitrate ( $\text{N-NO}_3^-$ ) levels reached or exceeded  $8 \text{ mg L}^{-1}$  in approximately 20% of the samples during the rainy season and 30% during the dry season. These values highlight the need for improved sanitation infrastructure to prevent further degradation of groundwater quality and to safeguard its suitability for human consumption.

Hydrogeochemical modeling has demonstrated that groundwater composition in the study area is primarily governed by silicate weathering and carbonate dissolution, with additional contributions from marine intrusion and human activities.

The methodological approach adopted in this study, which included sampling during contrasting seasonal periods, enabled the assessment of temporal variations in groundwater quality and the relative influence of environmental and anthropogenic factors. The integration of physicochemical analyses, X-ray diffraction of sediments and rocks, and geochemical modeling using Phreeqc provided a comprehensive understanding of the mineralogical and geochemical dynamics of the aquifer system. The application of Gibbs and Piper diagrams further supported the identification of dominant geochemical processes, such as precipitation, weathering and evaporation, and facilitated the classification of groundwater types based on ionic composition.

Thus, this research contributes both to the scientific understanding of hydrogeochemical processes in coastal aquifers and to the methodological advancement of integrated groundwater quality assessment, offering valuable insights for sustainable water resource management in coastal regions.

However, the study presents some limitations, particularly regarding the lack of a more comprehensive temporal analysis and the need for a more detailed assessment of anthropogenic sources of contamination. Future research is recommended to include continuous long-term monitoring and the integration of complementary tools, such as hydrogeological and isotopic modeling, as well as assessments of land use and land cover. These approaches will allow for a more integrated understanding of the factors influencing groundwater quality, contributing to more effective and sustainable management of the region's water resources.

## 5. DATA AVAILABILITY STATEMENT

Data availability not informed.

## 6. REFERENCES

- APHA; AWWA; WEF. **Standard Methods for the examination of water and wastewater**. 22nd ed. Washington, 2012. 1496 p.
- APPELO, C. A. J.; POSTMA, D. **Geochemistry, groundwater and pollution**. Leiden: A.A. Balkema, 2005. 558 p.



- BRAGA JÚNIOR, M. G.; MELO, J. G.; DINIZ FILHO, J. B. Comportamento hidrodinâmico e hidroquímico do sistema aquífero Barreiras-Jandaíra-Açu na área da Fazenda Belém, oeste da Bacia Potiguar, CE. **Águas Subterrâneas**, v. 31, n. 3, p. 222-242, 2017. <https://doi.org/10.14295/ras.v31i3.28674>
- BRASIL. Ministério da Saúde. **Portaria GM/MS nº 888, de 04 de maio de 2021**. Altera o Anexo XX da Portaria de Consolidação GM/MS nº 5, de 28 de setembro de 2017, para dispor sobre os procedimentos de controle e de vigilância da qualidade da água para consumo humano e seu padrão de potabilidade. Diário Oficial [da] União: seção 1, Brasília, DF, n. 85, p. 127, 07 de maio 2021.
- CELLIGOI, A. Considerações sobre análises químicas de águas subterrâneas. **Geografia**, v. 8, n. 1, p. 91-97, 1999. <https://doi.org/10.5433/2447-1747.1999v8n1p91>
- COETSIERS, M.; WALRAEVEN, K. Chemical characterization of the Neogene Aquifer, Belgium. **Hydrogeology Journal**, v. 14, p. 1556-1568, 2006. <https://doi.org/10.1007/s10040-006-0053-0>
- CUSTÓDIO, E.; LLAMAS, M. R. **Hidrologia Subterránea**. 2. ed. Barcelona: Omega, 1983. 1224 p.
- DEER, W. A.; HOWIE, R. A.; ZUSSMAN, J. **Uma introdução aos minerais constituintes das rochas**. 2. ed. Lisboa: Fundação Calouste Gulbenkian, 1992. 738 p.
- GARRELS, R. M.; CHRIST, C. L. **Solutions, Minerals and Equilibria**. San Francisco: W. H. Freeman, 1965. 450 p.
- GIBBS, R. J. Mechanisms controlling World Water Chemistry. **Science**, v. 170, n. 3962, p. 1088-1090, 1970. <https://doi.org/10.1126/science.170.3962.1088>
- GOMES, M. C. R.; MELO, D. H. C. T. B.; COSTA, M. S.; ANJOS, J. A. S. A.; TRINTA, M. M. A.; CAVALCANTE, I. N. Análise geoquímica das águas subterrâneas no município de Boquira, no semiárido baiano – Brasil. **Geochimica Brasiliensis**, v. 35, n. 1, p. 7-16, 2021. <https://doi.org/10.21715/GB2358-2812.2021351007>
- MAIA, S. R. R.; FREIRE, G. S. S.; GOMES, D. F.; ARAÚJO, K. V. Anomalias hidroquímicas nos aquíferos de Icapuí/CE: riscos à saúde da população. **Revista Ibero Americana de Ciências Ambientais**, v. 9, n. 2, p. 94-107, 2018. <https://doi.org/10.6008/CBPC2179-6858.2018.002.0009>
- MARASCHIN, A. J.; MIZUSAKI, A. M.; VASCONCELOS, P. M.; HINRICHS, R.; DE ROS, L. F.; ANJOS, S. M. C. Depositional age definition of the Açu Formation (Potiguar Basin, northeastern Brazil) through <sup>40</sup>Ar-<sup>39</sup>Ar dating of early-authigenic K-feldspar overgrowths. **Pesquisas em Geociências**, v. 37, n. 2, p. 85-96, 2010.
- MENTE, A. A. Água Subterrânea no Brasil. In: FEITOSA, F. A. C.; MANOEL FILHO, J.; FEITOSA, E. C.; DEMETRIO, J. G. A. (Orgs.). **Hidrogeologia: Conceitos e Aplicações**. 3. ed. Rio de Janeiro: CPRM; LABHID, 2008. p. 31-48.
- MOBÜS, G. **Qualigraf: software para interpretação de análises físico-químicas, versão Beta**. Fortaleza: FUNCEME, 2003.
- PARKHURST, D. L.; APPELO, C. A. J. **Description of input and examples for PHREEQC (version 3). A computer program for speciation, batch-reaction, one-dimensional transport, and inverse geochemical calculations**. Denver: USGS, 2013. 497 p.

- RICHTER, B. C.; KREITLER, C. W. **Geochemical techniques for identifying sources of groundwater salinization**. Boca Raton: CRC Press, 1993. 272 p.
- SERVIÇO GEOLÓGICO DO BRASIL. **Mapa Geodiversidade do Estado do Ceará, escala 1:750.000**. 2014. Available: <https://rigeo.sgb.gov.br/handle/doc/14692>. Access: 10 May 2021.
- SOARES, U. M.; ROSSETTI, E. L.; CASSAB, R. C. T. **Bacias sedimentares brasileiras: Bacia Potiguar**. Aracaju: Fundação Paleontológica Phoenix, 2003. v. 56. p. 1-10.
- SOUSA, D. C.; JARDIM DE SÁ, E. F.; VITAL, H.; NASCIMENTO, M. A. L. Falésias na Praia de Ponta Grossa, Icapuí, CE - Importantes deformações tectônicas cenozóicas em rochas sedimentares da Formação Barreiras. *In*: WINGE, M. *et al.* **Sítios Geológicos e Paleontológicos do Brasil**. Brasília: CPRM, 2009. v. 2. 515 p.
- SOUZA, D. P. **Estudo geoquímico-mineralógico de litologias aflorantes na orla litorânea de Icapuí – Ceará**. 2017. 81f. Dissertação (Mestrado em Geologia) – Programa de Pós-Graduação em Geologia, Universidade Federal do Ceará, Fortaleza, 2017.
- TUREKIAN, K. K.; WEDEPOHL, K. H. Distribution of the Elements in Some Major Units of the Earth's Crust. **Geological Society of America Bulletin**, v. 72, p. 175-192, 1961. [http://dx.doi.org/10.1130/0016-7606\(1961\)72\[175:DOTEIS\]2.0.CO;2](http://dx.doi.org/10.1130/0016-7606(1961)72[175:DOTEIS]2.0.CO;2)
- VENÂNCIO, L. O.; GOMES, D. F.; FREIRE, G. S. S.; LIMA NETO, I. O. Monitoramento da qualidade e hidrogeoquímica das águas subterrâneas do setor noroeste da região metropolitana de Fortaleza, CE. **Geochimica Brasiliensis**, v. 34, n. 2, p. 138-160, 2020. <https://doi.org/10.21715/GB2358-2812.2020342138>